

# Nanoscale

Accepted Manuscript



This is an *Accepted Manuscript*, which has been through the Royal Society of Chemistry peer review process and has been accepted for publication.

*Accepted Manuscripts* are published online shortly after acceptance, before technical editing, formatting and proof reading. Using this free service, authors can make their results available to the community, in citable form, before we publish the edited article. We will replace this *Accepted Manuscript* with the edited and formatted *Advance Article* as soon as it is available.

You can find more information about *Accepted Manuscripts* in the [Information for Authors](#).

Please note that technical editing may introduce minor changes to the text and/or graphics, which may alter content. The journal's standard [Terms & Conditions](#) and the [Ethical guidelines](#) still apply. In no event shall the Royal Society of Chemistry be held responsible for any errors or omissions in this *Accepted Manuscript* or any consequences arising from the use of any information it contains.

## Ultra-stretchable Conductors Based on Buckled Super-aligned Carbon Nanotube Films

Yang Yu,<sup>b</sup> Shu Luo,<sup>b</sup> Li Sun,<sup>a</sup> Yang Wu,<sup>a</sup> Kaili Jiang,<sup>a</sup> Qunqing Li,<sup>a</sup> Jiaping Wang,<sup>\*a</sup> and Shoushan Fan<sup>b</sup>

<sup>a</sup> *Department of Physics and Tsinghua-Foxconn Nanotechnology Research Center, Tsinghua University, Beijing 100084, China*  
*Collaborative Innovation Center of Quantum Matter, Beijing 100084, China*  
*\*E-mail: jpwang@tsinghua.edu.cn*

<sup>b</sup> *Department of Physics and Tsinghua-Foxconn Nanotechnology Research Center*  
*School of Materials Science and Engineering*  
*Tsinghua University, Beijing 100084, China*

Ultra-stretchable conductors are fabricated by coating super-aligned carbon nanotube (SACNT) films on pre-strained polydimethylsiloxane (PDMS) substrates and forming buckled SACNT structures on PDMS after release of the pre-strain. The parallel SACNT/PDMS conductors demonstrate excellent stability with normalized resistance changes of only 4.1% under an applied strain as high as 200%. The SACNT/PDMS conductors prepared with cross-stacked SACNT films show even lower resistance variation. The parallel SACNT/PDMS conductors exhibit high durability with resistance increase of less than 5% after 10,000 cycles at 150% strain. *In situ* microscopic observations demonstrate that the buckled SACNT structures are straightened during the stretching process with reversible morphology evolution and thus the continuous SACNT conductive network can be protected from fracture. Due to the excellent electrical and mechanical properties of SACNT films and the formation of the buckled structure, SACNT/PDMS films exhibit high stretchability and durability, possessing great potential for uses as ultra-stretchable conductors for wearable electronics, sensors, and energy storage devices.

## 1. Introduction

With the increasing development of stretchable electronics, conductors that can remain electrically conductive under large strains become quite critical for many new applications such as stretchable energy devices and human-motion sensors.<sup>[1-3]</sup> Many stretchable material structures such as wavy metal films, carbon nanotube/polymer composite films, and graphene/polymer composite films have been developed that demonstrate excellent conductivity and mechanical robustness by the design of the wave-like or net-shaped structures.<sup>[4-9]</sup> Carbon nanotube (CNT) is considered as one of the promising materials for stretchable conductors due to its large aspect ratio, excellent electrical conductivity, high thermal stability, and mechanical robustness.<sup>[10-12]</sup> Many stretchable conductors based on CNT/polymer composites have been reported in literature.<sup>[13-16]</sup> In these composite structures, CNTs form a continuous and conductive network, and the polymer matrix offers excellent stretchability and protects the CNT network from fracture. Typical CNT/polymer stretchable structures reported so far include rubberlike conductive composite with uniform dispersion of single-walled CNTs (SWCNT) in a polymer matrix,<sup>[13]</sup> transparent and conductive film with randomly distributed CNTs sprayed on a stretchable polymer film,<sup>[14]</sup> and buckled electrode fabricated by laminating a randomly oriented SWCNT film on a pre-strained polydimethylsiloxane (PDMS) substrate.<sup>[15, 16]</sup> Although high conductivity and stretchability were demonstrated in these structures, there still exist several limitations for practical applications, such as complicated fabrication process, deteriorated conductivity under large applied strain, and poor durability. In these composites, CNTs were randomly oriented with weak bonding among tubes and the CNT junctions may fracture under large applied strains and cause resistance increase. Repeated tensile loading may further break the CNT junctions

and result in more resistance variation. Therefore, the randomly oriented CNT films may not be the best choice for stretchable conductors.

Super-aligned CNTs (SACNTs) attract much attention these years.<sup>[17, 18]</sup> Ultrathin and continuous SACNT films can be easily drawn from SACNT arrays by an end-to-end joining mechanism, which is cost-effective and environmentally benign. The alignment of CNTs in the SACNT film is parallel to the drawing direction. The SACNT films are freestanding, lightweight, and possess excellent electrical and mechanical properties along their axial direction.<sup>[19, 20]</sup> By cross-stacking SACNT layers, SACNT films with isotropic electrical conductivity can be obtained. The thickness of the SACNT film depends on the numbers of CNT layers. SACNT films have been widely used in loudspeakers,<sup>[21]</sup> touch screens,<sup>[22]</sup> electrodes for lithium ion batteries,<sup>[23-25]</sup> current collectors,<sup>[26, 27]</sup> and so on.

In this work, high performance SACNT/PDMS stretchable conductors were fabricated by coating parallel or cross-stacked SACNT films on a flexible and pre-strained PDMS substrate. Buckled SACNT structures were formed on the PDMS substrate after release of the pre-strain. *In situ* microscopic observation demonstrated that the buckled SACNT structures were straightened during the stretching process with reversible morphology evolution and thus the SACNT conductive network could be protected from fracture. The SACNT/PDMS conductors remained highly conductive under an applied strain as high as 200% and withstood 10,000 stretching-releasing cycles at 150% strain with a resistance change less than 5%. The excellent stretchability and durability of the SACNT/PDMS conductive films are of great advantages over other carbon-based stretchable conductors reported in literature.<sup>[13-15]</sup>

## 2. Results and Discussion

### 2.1. Formation and resistance changes of the buckled SACNT/PDMS films

The fabrication processes of the buckled SACNT/PDMS conductors are schematically shown in Figure 1a. Firstly, a PDMS substrate with a length of  $L$  is pre-strained to a length of  $L+\Delta L$ . Secondly, a continuous SACNT film is directly drawn from SACNT arrays on a Si wafer (Figure 1b) and various layers of the SACNT films are then stacked onto the pre-strained PDMS substrate. Figure 1c shows the scanning electron microscopy (SEM) image of an SACNT film, where parallel SACNT bundles can be clearly observed. After the PDMS substrate is released to its original length  $L$ , buckled SACNT structures are formed on the PDMS substrate (Figure 1d). The inset of Figure 1a is the photograph of a highly flexible SACNT/PDMS composite film with buckled structure.

Buckled SACNT/PDMS conductors with various layers of SACNT films were fabricated. The PDMS substrates were first stretched to a pre-strain of 40%. 2, 6, and 10 layers of SACNT films were then stacked onto the pre-strained PDMS substrates. After release of the pre-strain, buckled SACNT/PDMS composite films were obtained. Tensile strain was applied using an Instron 5848 microtester and the resistance changes of the SACNT/PDMS films under applied strains up to 60% were monitored by a Keithley 2400 Source Meter at the same time. The sheet resistance of a single layer of the SACNT film along the drawing direction is about  $1000 \Omega \text{ sq}^{-1}$  [22]. As the number of the SACNT layers increased from 2 to 6 and 10, the initial resistances of the SACNT/PDMS composites decreased from 684 to 430 and 186  $\Omega$  (Figure S1). The normalized resistance changes ( $\Delta R/R_0$ ) of these SACNT/PDMS films as a function of the applied strain are plotted in Figure 2. The resistances of the SACNT/PDMS composites with 2 and 6 layers of SACNT films kept almost constant when the applied tensile strain was smaller than the value of the pre-strain at 40%. After the applied strain exceeded 40%, the

normalized resistance changes ( $\Delta R/R_0$ ) gradually increased to 19% and 23% at 50% strain for the composites with 2 and 6 layers of SACNT films. For the SACNT/PDMS composite with 10 layers of SACNT films, although it showed the lowest initial resistance, a sharp increase of resistance occurred when the applied strain exceeded the level of pre-strain at 40%. The normalized resistance changes ( $\Delta R/R_0$ ) increased dramatically to 125% at 50% strain due to the detached SACNT conductive bundles especially the top layers that have poor interaction with the surface of the PDMS substrate, as shown in Figure S2. Comparing the SACNT/PDMS composites with different layers of SACNT films, the 6-layer SACNT/PDMS composites demonstrated both relatively low initial resistance and stability in enduring strains larger than the level of pre-strain, thus are more suitable for use in real stretchable devices. The experiments and analyses below are all based on the SACNT/PDMS conductors with 6 layers of SACNT films.

SACNT/PDMS composites were also prepared with larger pre-strains of the PDMS substrate in order to obtain stretchable conductors that can remain a constant conductivity under larger applied strains. Figure 3a shows the relationship between normalized resistance changes ( $\Delta R/R_0$ ) and the applied strain in the SACNT/PDMS composites with no pre-strain, 40%, and 200% pre-strain. The SACNT/PDMS film with no pre-strain showed sharp resistance increase during stretching with normalized resistance increase of 632% at 40% strain, and such increase in resistance was irreversible. As shown in Figure 3b, after the SACNT/PDMS film with no pre-strain was loaded to 10% and 20% strains, upon unloading, the resistance could not recover to its original value, and the normalized resistance changes were around 20% and 80% respectively. In contrast, the SACNT/PDMS composites with pre-strains exhibited much more stable resistances when the applied strain was smaller than the level of pre-strain. For the SACNT/PDMS film with 40% pre-strain, the normalized resistance change was only 4% at 40% strain. The sample with 200% pre-strain could even withstand a strain as large as

200% with a normalized resistance change of only 4.1%. Moreover, the resistance changes of the SACNT/PDMS films with pre-strain sample were fully reversible as long as the applied strain was smaller than the value of pre-strain. As shown in Figure 3b, the resistance of the SACNT/PDMS films with 40% pre-strain almost recovered to its original value when the sample was loaded to 40% strain and then released to its original length. After the applied strain was increased to a value larger than the pre-strain, the resistance increased irreversibly. When the SACNT/PDMS film with 40% pre-strain was loaded with a 50% strain, the normalized resistance increase reached 20%. Such increased resistance remained after the sample was unloaded, similar to SACNT/PDMS film with no pre-strain.

## 2.2. *In situ* SEM observation of the buckled SACNT structures

A lab-designed tensile module was used to stretch the SACNT/PDMS composites within the SEM chamber to make *in situ* observation of the dynamic changes of the surface morphologies during the loading and releasing cycles. The morphologies of the SACNT/PDMS film with no pre-strain at its original stage and at 40% and 60% strains during the stretch process are shown in Figure 4a. At the original stage, the SACNT films uniformly covered the PDMS substrate. At 40% strain, the SACNT bundles began to break and large gaps could be observed. Such gaps became wider when the strain was further increased to 60%. The fracture of SACNT films resulted in the sharp and irreversible increase in resistance, as shown in Figures 3a and 3b.

In comparison, the formation and straightening of the wavy structures of the SACNT/PDMS film with 40% pre-strain during the release of the pre-strain and the following stretch process were revealed in sequences by *in situ* SEM observation (Figure 4b). Firstly, the SACNT film was stacked on the PDMS substrate with 40% pre-strain (Figure 4b(i)). The surface was smooth with straight and aligned SACNT bundles. Afterwards, the PDMS substrate was

partially released to 20% strain and then to its original length. The SACNT film was compressed during the release of the PDMS substrate, meanwhile wavy and buckled structures of the SACNT films gradually formed on the PDMS substrate (Figure 4b(ii)). Such buckled CNT structures were also reported in literature and a buckling mechanism was proposed by considering the interaction among CNT bundles and the adhesion between CNTs and the substrate.<sup>[9]</sup> These buckled structures are out of the PDMS surface. Part of the CNT bundles adhered on the PDMS surface via the van der Waals force and the other part suspended in air, so the SACNT films detached from the PDMS substrate periodically, as shown in Figure S3. After the full release of the pre-strain, strains of 20%, 40%, and 60% were applied to the buckled SACNT/PDMS composites along the direction of the pre-strain. During the stretch process, the wavy SACNT structures became gradually straightened. When the SACNT/PDMS composite were loaded with a strain equal to the value of pre-strain, i.e., 40%, the wavy structures were almost flattened (Figure 4b(v)). The continuous and conductive SACNT network still remained intact without fracture of SACNTs. The integrity of the SACNT conductive network contributed to the steady resistance with only 4% normalized increase for the pre-strained SACNT/PDMS composite at applied strains smaller than the value of pre-strain (Figure 3). In addition, as the buckling and straightening processes were reversible, the resistance of the SACNT/PDMS composite could be fully recovered to the original value upon unloading. As the applied strain was increased further to 60%, exceeding the pre-strain, the wavy structures became totally flattened and gaps perpendicular to the direction of applied strain appeared, leading to the fracture of the SACNT films, as marked by the arrow in Figure 4b(vi). The breakdown of the conductive SACNT network was responsible for the rapid and irreversible increase of the resistance at strains larger than the pre-strain in Figure 3b (20% normalized resistance increase at 60% strain).



### 2.3. Cross-stacked SACNT/PDMS conductors

Cross-stacked SACNT films have isotropic electrical properties and have been widely used as conductors.<sup>[17]</sup> SACNT/PDMS composites were prepared by cross-stacking 6 layers of SACNT films on the pre-strained PDMS substrates, and their performances as stretchable conductors were compared with the SACNT/PDMS composites with parallel SACNT films. The initial resistance of the cross-stacked SACNT/PDMS composite was 497  $\Omega$ , which was slightly larger than that of the parallel SACNT/PDMS composite with the same layers of SACNT films (430  $\Omega$ ). Figure 5a shows the normalized resistance changes as a function of the applied strain for the 40% pre-strained SACNT/PDMS composites with parallel and cross-stacked SACNT films (denoted as “||” and “ $\perp$ ” CNT films). The normalized resistance increase was only 1.7% at a 40% strain for the cross-stacked SACNT/PDMS composite, which presented a more constant resistance than the parallel SACNT/PDMS composite with 4% resistance change at the same strain. Especially, at strains larger than the pre-strain (40%), the normalized resistance increase of the cross-stacked SACNT/PDMS composite was much smaller than the parallel SACNT/PDMS composite. When the applied strain increased to 60%, the normalized resistance increase of the cross-stacked SACNT/PDMS composite was 18%, compared with a much larger increase of about 80% for the parallel SACNT/PDMS composite.

Figure 5b shows the normalized resistance changes of the cross-stacked SACNT/PDMS films with different pre-strains from 0 to 40% as a function of the applied strain. Note that the cross-stacked SACNT/PDMS films were only pre-strained up to 40%. As the pre-strain increased to 60%, due to the lateral broadening of the PDMS substrate during the release of the pre-strain, the SACNT bundles aligned perpendicular to the tensile direction would suffer from tension stress. Some of these SACNT bundles fractured and resulted in large-area

delamination of the SACNT film from the PDMS substrate and failure of the composite, as shown in Figure S4. Therefore, the value of pre-strain for the cross-stacked SACNT/PDMS films was limited to 40%. The trend of resistance variation with applied strain was similar to that in the parallel SACNT/PDMS films. The resistance of the SACNT/PDMS film with no pre-strain increased rapidly as the strain increased. But for the SACNT/PDMS films with pre-strains, when the applied strain was smaller than the pre-strain, the resistance kept almost constant. When the applied strain was larger than the pre-strain, the resistance began to increase rapidly. *In situ* SEM images in Figure 5c show the wavy cross-stacked SACNT structures on a 40% pre-strained substrate and the morphology evolution at applied strains of 40% and 80%. As the applied strain increased, the buckled SACNT structures were straightened gradually, similar to the parallel SACNT/PDMS films. When the applied strain was as high as 80%, exceeding the value of pre-strain at 40%, the cross-stacked SACNT films presented different features compared with the parallel SACNT films. Though the SACNT bundles along the direction of the tensile loading were fractured marked by the arrow in Figure 5c (iii), the SACNT bundles aligned perpendicular to the tensile direction could still act as “electric bridges” to connect the gaps formed by the broken SACNT bundles along the tensile direction. Consequently, the conductive path could still be maintained in the SACNT/PDMS film, leading to the more gentle resistance increase than that of the parallel SACNT/PDMS film as shown in Figure 5a. The extreme low resistance variation of the cross-stacked SACNT/PDMS composite is beneficial for applications of resistance-sensitive devices such as stretchable conductors that are integrated with sensors.

The stretchable SACNT/PDMS conductors prepared in this work possess both excellent stretchability and resistance stability, compared with other carbon-based stretchable conductors reported in literature.<sup>[8, 9, 13, 15, 28-31]</sup> As shown in Figure 6, the SACNT/PDMS

ultra-stretchable conductors exhibit the lowest resistance variation at the largest applied strain. The parallel SACNT/PDMS conductors can endure an applied strain as high as 200% with a normalized resistance increase of only 4.1%. The resistance of the cross-stacked SACNT/PDMS conductors can be maintained almost constant with a resistance change of only 1.7% at 40% strain. Such impressive performance could be attributed to the unique characteristics of the SACNT films. SACNT films with highly oriented SACNT bundles provide a conductive and robust network in the composite. Therefore the SACNT/PDMS films are highly flexible and conductive, which ensure the wavy structures to be fully recovered during the loading-unloading cycles. The continuous SACNT films remain intact at large strains below the value of the pre-strain that results in low resistance variation and high stretchability.

#### **2.4. Durability of the SACNT/PDMS conductors**

The durability of the parallel SACNT/PDMS conductor was characterized by performing cyclic tensile tests with 150% strain for 10,000 cycles and the resistance of the sample was monitored at each cycle. Figure 7 shows the normalized resistance changes of the parallel SACNT/PDMS films with no pre-strain and with 200% pre-strain during the 10,000 cycles with 150% strain. The pre-strained SACNT/PDMS film demonstrated steady resistance during the cyclic tensile loading. Even after 10,000 cycles, the normalized resistance increase was still less than 5%. As a contrast, the resistance of the SACNT/PDMS film with no pre-strain was about 45 times its original value after the first cycle, and such large resistance remained during the following cycles. Figure S5 shows the durability of a cross-stacked PDMS/SACNT film with 40% pre-strain for 10,000 cycles at 40% strain. The normalized resistance increase was about 7.5% after 10,000 cycles, which was larger than that of the parallel SACNT/PDMS films. In the cross-stacked PDMS/SACNT film, SACNT bundles aligned perpendicular to the tensile direction suffered from cyclic tensile stress during the

unloading processes due to the lateral broadening of the PDMS substrate. Fracture of these SACNT bundles resulted in the resistance increase and thus affected the durability of the cross-stacked PDMS/SACNT film.

The morphologies of the parallel SACNT/PDMS films with no pre-strain and with 200% pre-strain were examined by SEM before and after the cyclic tensile testing. For the sample with no pre-strain, the SACNT bundles were broken and huge gaps formed under an applied strain of 40% (Figure 8a), leading to the dramatic increase in resistance. Such gaps could not be recovered during the unloading process, therefore such resistance increase was irreversible in the following cycles. However, for the pre-strained SACNT/PDMS films, the buckled SACNT structures could be straightened and formed repeatedly without fracture of the conductive SACNT network (Figure 8b). No evident structural failures were present in the pre-strained sample after 10,000 tensile cycles except very small gaps perpendicular to the tensile direction caused by the repeated loading-unloading processes. These results further demonstrate the strong interaction between the SACNT bundles and the PDMS substrate that can assure the structural stability of the SACNT/PDMS films for 10,000 cycles. Due to the excellent mechanical performance and recovery capability of the SACNT films at strains below the pre-strain, the continuous SACNT conductive network could be well maintained. Thus ultra-high durability was achieved in the pre-strained SACNT/PDMS films with almost constant resistance during the long-term loading cycles. The high durability of the SACNT/PDMS films is of great value for use in stretchable devices.

Finally, in order to test the practical performance of the SACNT/PDMS stretchable conductor, a series circuit was constructed that connected an LED with the SACNT/PDMS film prepared with a pre-strain of 100% and a Keithley source meter with stabilized output of 10 V. Figure 9a shows a photograph of the illuminated LED without applying any strain. Afterwards, the

SACNT/PDMS composite film was stretched to a 100% strain by a microtester, and the LED did not show any noticeable luminance fluctuation as shown in Figure 9b, revealing that the resistance change of the SACNT/PDMS conductor was ignorable during stretching. In order to improve the anti-scratch properties of the SACNT/PDMS conductors in various applications, a thin layer of PDMS was spin-coated on the buckled SACNT/PDMS films to prevent damage from exterior physical contacts. The initial resistance of the SACNT/PDMS films remained almost constant after the spin-coating process. The normalized resistance increase of the spin-coated SACNT/PDMS composite during stretching was comparable with those without the spin-coating process. Combining the advantages of the facile fabrication and high stretchability and excellent durability, the SACNT/PDMS films demonstrate great potential as ultra-stretchable conductors in flexible electronics.

### 3. Conclusion

Ultra-stretchable SACNT/PDMS conductors are fabricated by stacking parallel or cross-stacked SACNT films onto pre-strained PDMS substrates and forming wavy buckled SACNT structures after the release of the pre-strain. The parallel SACNT/PDMS conductors can be stretched to 200% strain with a normalized resistance increase of only 4.1%. The cross-stacked SACNT/PDMS conductors exhibit even lower resistance variation, with 1.7% resistance change at 40% strain. The parallel SACNT/PDMS conductors exhibit high durability with resistance increase of less than 5% after 10,000 cycles at 150% strain. *In situ* microscopic observations reveal the formation and straightening of the buckled SACNT structures during the loading and releasing processes with reversible morphology evolution, and the SACNT conductive network can be protected from fracture. The excellent stretchability and resistance stability and high durability of the SACNT/PDMS composite conductors may find broad applications in stretchable interconnections and power devices.

**Acknowledgements**

This work was supported by the National Basic Research Program of China (2012CB932301), NSFC (51102146 and 51472141), and the NCET Program of China.

**Notes and References**

- 1 S. Xu, Y. Zhang, J. Cho, J. Lee, X. Huang, L. Jia, J. A. Fan, Y. Su, J. Su, H. Zhang, H. Cheng, B. Lu, C. Yu, C. Chuang, T.-i. Kim, T. Song, K. Shigeta, S. Kang, C. Dagdeviren, I. Petrov, P. V. Braun, Y. Huang, U. Paik, J. A. Rogers, *Nature Communications* 2013, **4**, 1543.
- 2 C. Wang, W. Zheng, Z. Yue, C. O. Too, G. G. Wallace, *Advanced Materials* 2011, **23**, 3580.
- 3 T. Yamada, Y. Hayamizu, Y. Yamamoto, Y. Yomogida, A. Izadi-Najafabadi, D. N. Futaba, K. Hata, *Nature Nanotechnology* 2011, **6**, 296.
- 4 D. Y. Khang, H. Q. Jiang, Y. Huang, J. A. Rogers, *Science* 2006, **311**, 208.
- 5 S. p. P. r. Lacour, S. Wagner, Z. Huang, Z. Suo, *Applied Physics Letters* 2003, **82**, 2404.
- 6 D.-Y. Khang, J. A. Rogers, H. H. Lee, *Advanced Functional Materials* 2009, **19**, 1526.
- 7 D. H. Kim, R. Ghaffari, N. Lu, J. A. Rogers, *Annual Review of Biomedical Engineering* 2012, **14**, 113.
- 8 Z. Chen, W. Ren, L. Gao, B. Liu, S. Pei, H.-M. Cheng, *Nature Materials* 2011, **10**, 424.
- 9 F. Xu, X. Wang, Y. Zhu, Y. Zhu, *Advanced Functional Materials* 2012, **22**, 1279.
- 10 M. F. Yu, O. Lourie, M. J. Dyer, K. Moloni, T. F. Kelly, R. S. Ruoff, *Science* 2000, **287**, 637.
- 11 T. W. Ebbesen, H. J. Lezec, H. Hiura, J. W. Bennett, H. F. Ghaemi, T. Thio, *Nature* 1996, **382**, 54.
- 12 H. J. Dai, *Surface Science* 2002, **500**, 218.
- 13 T. Sekitani, Y. Noguchi, K. Hata, T. Fukushima, T. Aida, T. Someya, *Science* 2008, **321**, 1468.
- 14 L. Hu, W. Yuan, P. Brochu, G. Gruner, Q. Pei, *Applied Physics Letters* 2009, **94**, 161108.
- 15 C. Yu, C. Masarapu, J. Rong, B. Wei, H. Jiang, *Advanced Materials* 2009, **21**, 4793.

- 16 Z. Niu, H. Dong, B. Zhu, J. Li, H. H. Hng, W. Zhou, X. Chen, S. Xie, *Advanced Materials* 2013, **25**, 1058.
- 17 K. L. Jiang, J. P. Wang, Q. Q. Li, L. A. Liu, C. H. Liu, S. S. Fan, *Advanced Materials* 2011, **23**, 1154.
- 18 K. L. Jiang, Q. Q. Li, S. S. Fan, *Nature* 2002, **419**, 801.
- 19 X. B. Zhang, K. L. Jiang, C. Teng, P. Liu, L. Zhang, J. Kong, T. H. Zhang, Q. Q. Li, S. S. Fan, *Advanced Materials* 2006, **18**, 1505.
- 20 K. Liu, Y. H. Sun, L. Chen, C. Feng, X. F. Feng, K. L. Jiang, Y. G. Zhao, S. S. Fan, *Nano Letters* 2008, **8**, 700.
- 21 L. Xiao, Z. Chen, C. Feng, L. Liu, Z. Q. Bai, Y. Wang, L. Qian, Y. Y. Zhang, Q. Q. Li, K. L. Jiang, S. S. Fan, *Nano Letters* 2008, **8**, 4539.
- 22 C. Feng, K. Liu, J. S. Wu, L. Liu, J. S. Cheng, Y. Y. Zhang, Y. H. Sun, Q. Q. Li, S. S. Fan, K. L. Jiang, *Advanced Functional Materials* 2010, **20**, 885.
- 23 Y. Wu, Y. Wei, J. Wang, K. Jiang, S. Fan, *Nano Letters* 2013, **13**, 818.
- 24 X. He, Y. Wu, F. Zhao, J. Wang, K. Jiang, S. Fan, *Journal of Materials Chemistry A* 2013, **1**, 11121.
- 25 S. Luo, H. Wu, Y. Wu, K. Jiang, J. Wang, S. Fan, *Journal of Power Sources* 2014, **249**, 463.
- 26 K. Wang, S. Luo, Y. Wu, X. He, F. Zhao, J. Wang, K. Jiang, S. Fan, *Advanced Functional Materials* 2013, **23**, 846.
- 27 Y. Wu, H. Wu, S. Luo, K. Wang, F. Zhao, Y. Wei, P. Liu, K. Jiang, J. Wang, S. Fan, *Rsc Advances* 2014, **4**, 20010.
- 28 L. Cai, J. Li, P. Luan, H. Dong, D. Zhao, Q. Zhang, X. Zhang, M. Tu, Q. Zeng, W. Zhou, S. Xie, *Advanced Functional Materials* 2012, **22**, 5238.
- 29 K. Liu, Y. Sun, P. Liu, X. Lin, S. Fan, K. Jiang, *Advanced Functional Materials* 2011, **21**, 2721.



- 30 K. H. Kim, M. Vural, M. F. Islam, *Advanced Materials* 2011, **23**, 2865.
- 31 M. K. Shin, J. Oh, M. Lima, M. E. Kozlov, S. J. Kim, R. H. Baughman, *Advanced Materials* 2010, **22**, 2663.

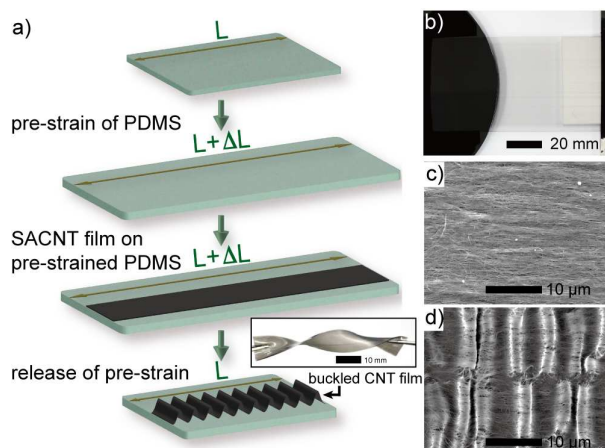


**Figure 1.** (a) Schematic processes for fabricating a buckled SACNT/PDMS conductor and photograph of a flexible sample; (b) photograph and (c) SEM image of an SACNT film; (d) SEM image of the buckled SACNT structures on a pre-strained PDMS substrate.

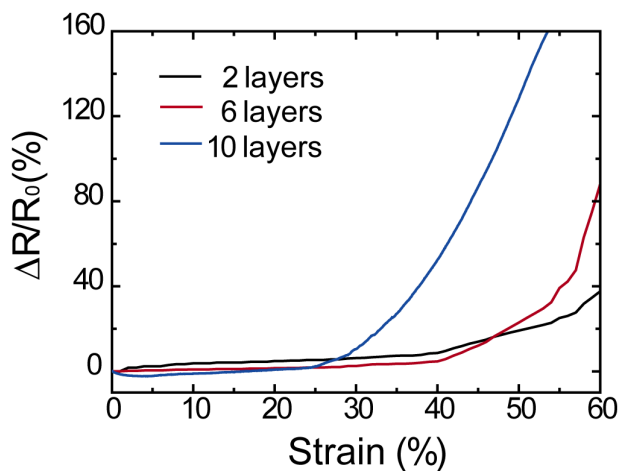


**Figure 2.** Normalized resistance changes of the 40% pre-strained SACNT/PDMS conductors with 2, 6, and 10 layers of SACNT films as a function of the applied tensile strain.

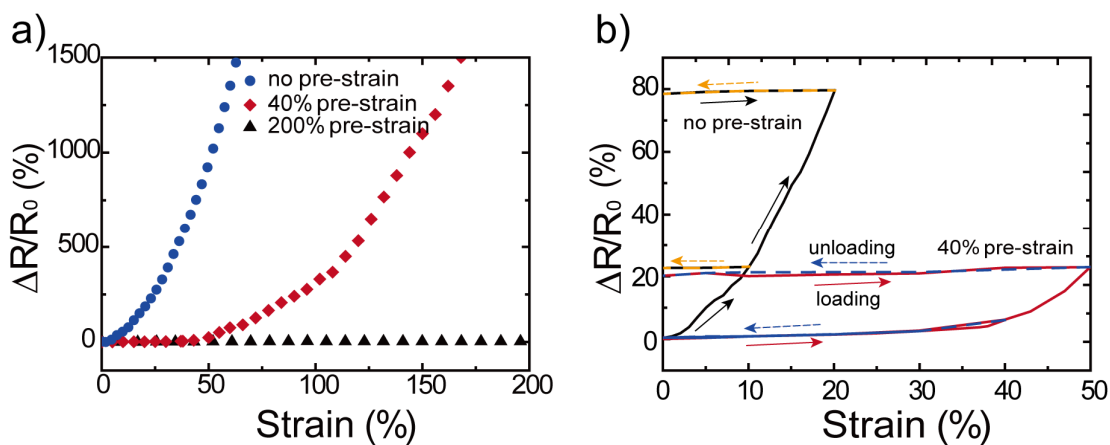


**Figure 3.** Normalized resistance changes of the SACNT/PDMS films (a) with different pre-strains as a function of the applied tensile strain; (b) with no pre-strain and 40% pre-strain during loading-unloading cycles (loading: solid lines; unloading: dashed lines).

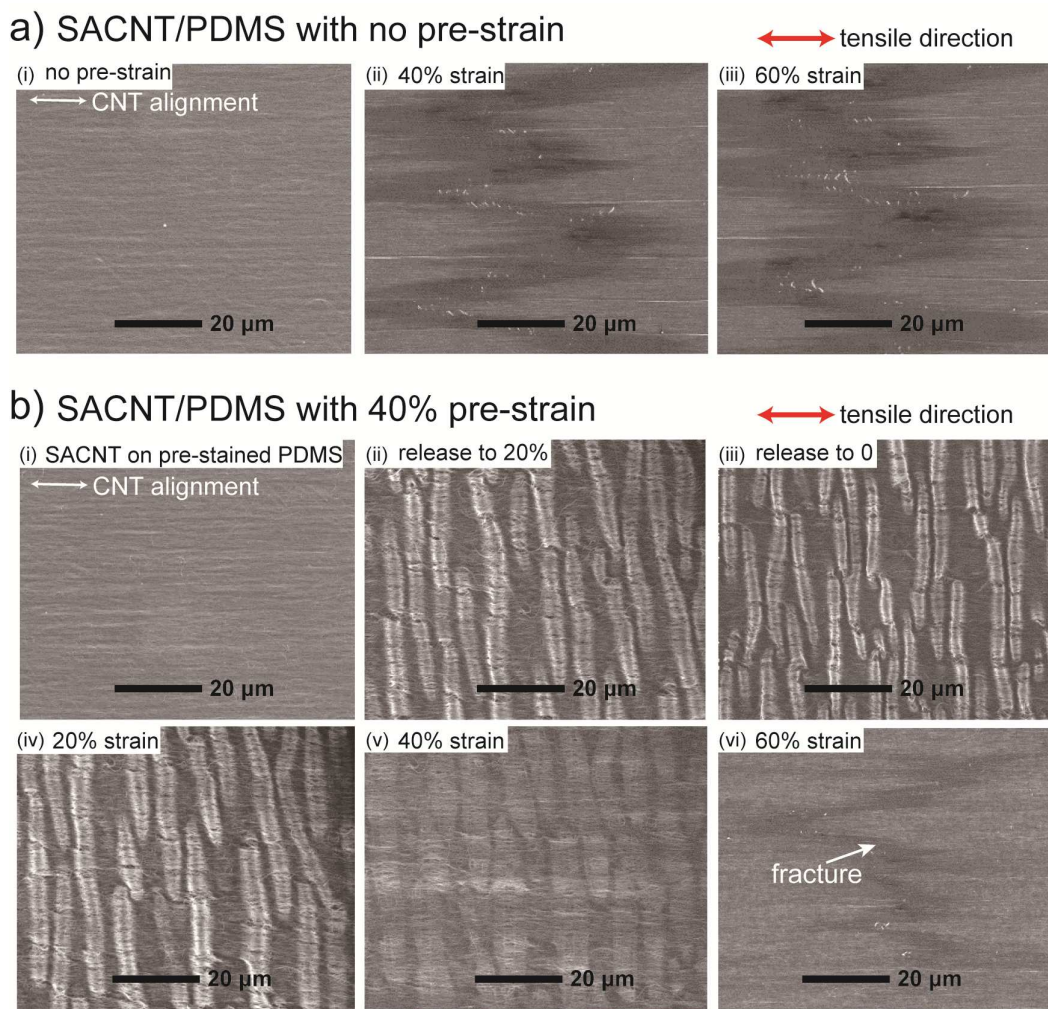


**Figure 4.** *In situ* SEM images of (a) the SACNT/PDMS film with no pre-strain during stretching; (b) the SACNT/PDMS film with 40% pre-strain during the release of the pre-strain and further stretch.

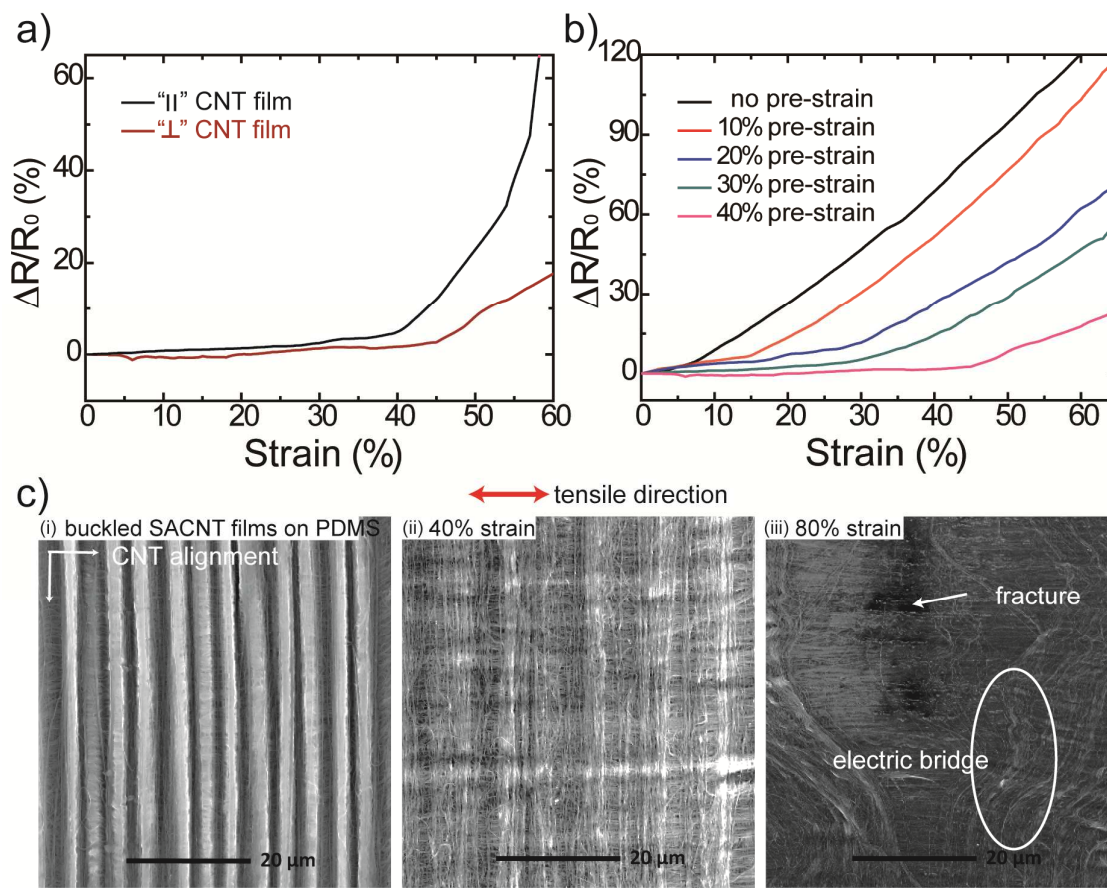


**Figure 5.** (a) Normalized resistance changes of the 40% pre-strained parallel and cross-stacked SACNT/PDMS films as a function of the applied tensile strain; (b) Resistance variations of the cross-stacked SACNT/PDMS films prepared with different pre-strains; (c) *In situ* SEM images of the wavy cross-stacked SACNT structures and the morphology evolution at applied strains of 40% and 80%.

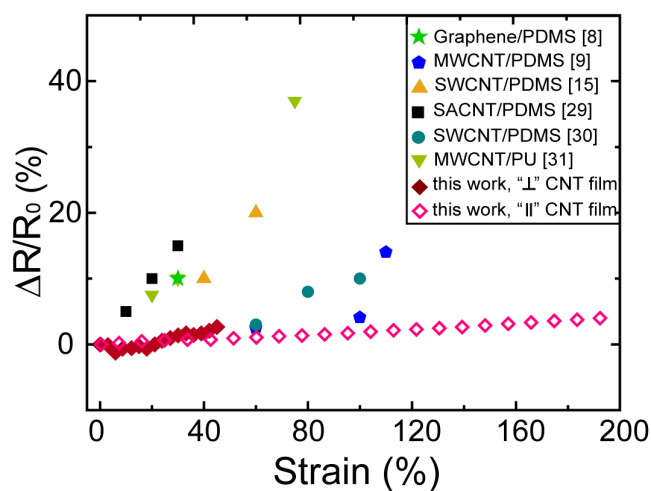


**Figure 6.** Comparison of the stretchability and resistance stabilities between this work and other stretchable conductors based on carbon materials reported in literature.

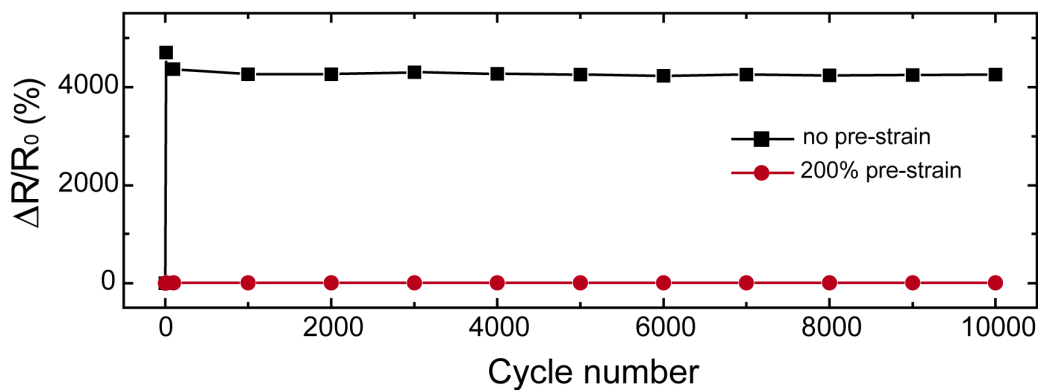
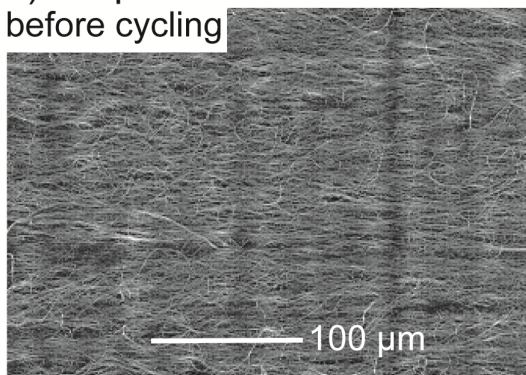
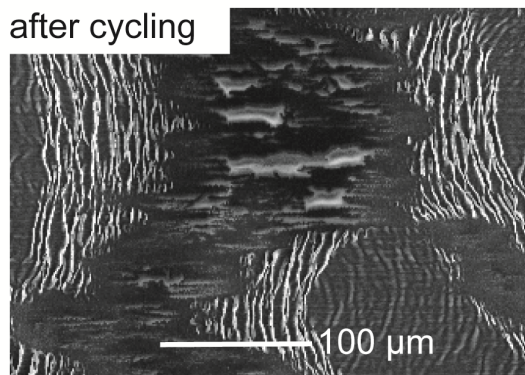


**Figure 7.** Normalized resistance changes of the parallel SACNT/PDMS films with no pre-strain and 200% pre-strain during 10,000 cycles at 150% strain.

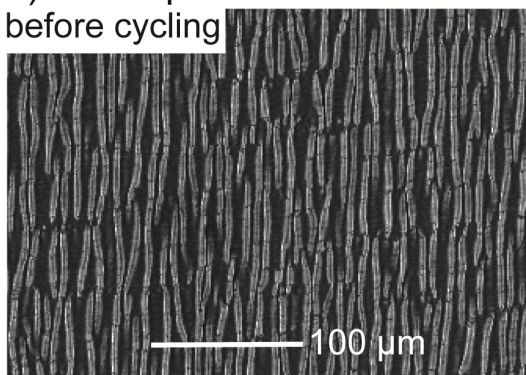
a) No pre-strain  
before cycling



after cycling



b) 200% pre-strain  
before cycling



after cycling

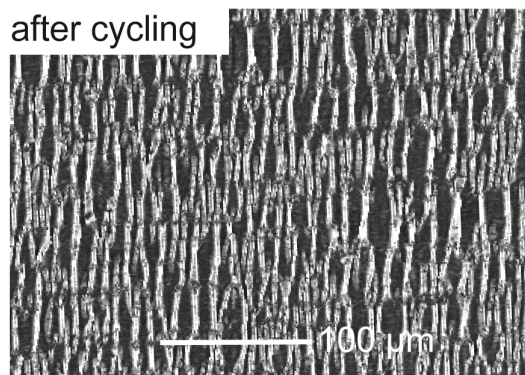


**Figure 8.** SEM images of the SACNT/PDMS films (a) with no pre-strain and (b) with 200% pre-strain before and after 10,000 tensile cycles at 150% strain.

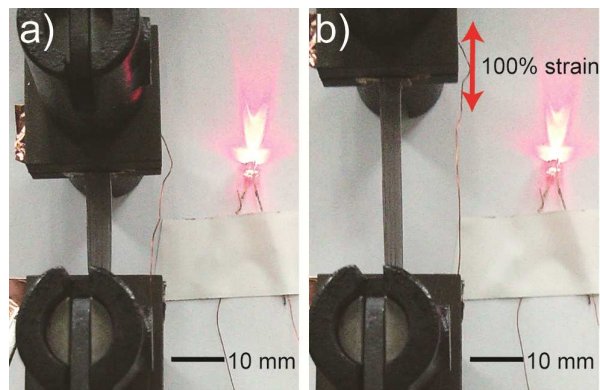


**Figure 9.** a) An illuminated LED in a circuit connected with a SACNT/PDMS conductor; b) Photograph of the LED under an applied strain of 100%.

### ToC

Buckled SACNT/PDMS conductors are fabricated by coating SACNT films on pre-strained PDMS that exhibit high stretchability, resistance stability, and durability.

